Reconstitution of functional UCP1 using CRISPR/Cas9 in the white adipose tissue of pigs decreases fat deposition and improves thermogenic capacity

Qiantao Zheng[1,5,†], Jun Lin[1,†], Jiaojiao Huang[1,5,†], Xueying Zhang[2], Rui Zhang[1,5], Chunwei Cao[1,5], Catherine Hambly[3], Hongyong Zhang[1,5], Qitao Ji[1,5], Xiao Wang[1,5], Guosong Qin[1,5], John R. Speakman[2,3], Yanfang Wang[4,§], Wanzhu Jin[1,5,§], Jianguo Zhao[1,5,§]

Affiliations:

[1]Institute of Zoology, Chinese Academy of Sciences, Beijing100101, China,

[2] Institute of Genetics and Developmental Biology, Chinese Academy of Sciences, Beijing100101, China,

[3] University of Aberdeen

[4]Institute of Animal Sciences, Chinese Academy of Agricultural Sciences, Beijing 100193, China,

[5] Savaid Medical School, University of Chinese Academy of Sciences, Beijing 100049, China,

[†]These authors contributed equally to this work

[§]Correspondence and requests for materials should be addressed to J. Zhao, W. Jin and Y. Wang.

zhaojg@ioz.ac.cn;

Jinw@ioz.ac.cn

Wangyanfang@caas.cn

Abstract

Uncoupling protein 1 (*UCP1*), localized on the inner mitochondrial membrane, generates heat via uncoupling the movement of protons across the inner membrane from synthesis of ATP. It is a key element of non-shivering thermogenesis and probably regulation of body adiposity. Pigs (Artiodactyl family *Suidae*) lack a functional *UCP1* gene, resulting in poor thermoregulatory ability and susceptibility to cold, which is an economic and welfare issue due to neonatal mortality. Pigs also have a tendency to fat accumulation, which may also be linked to their lack of UCP1, andinfluences the efficiency of pig production. Here, we report the first application of a CRISPR/Cas9 mediated homologous recombination (HR) independent approach to efficiently insert Adiponectin-*UCP1* into the porcine endogenous *UCP* locus. The resultant *UCP1* knock in (KI) pigs showed improved ability to maintain body temperature during acute cold exposure, but did not show alterations in physical activity levels and total daily energy expenditure. Further, ectopic expression of *UCP1* in white adipose tissue (WAT) dramatically decreased fat deposition (5% less, $P<0.01$) and increased lean body mass ($P<0.05$) without affecting the overall growth rate and food conversion efficiency. Mechanistic studies indicated that the loss of fat upon activation of *UCP1* in WAT was linked to elevated lipolysis. *UCP1* KI pigs are a potentially valuable resource for the pig industry, combining cold adaptation, which improves pig welfare and reduces economic losses, with reduced fat deposition and higher lean meat product.

Key words: *UCP1*, thermoregulation, fat deposition, pig, CRISPR/Cas9

Introduction

Uncoupling protein 1 (*UCP1*) serves as a proton leak across the inner mitochondrial membrane, contributing to energy dissipation as heat, and hence plays the key role in brown adipose tissue (BAT) mediated adaptive non-shivering thermogenesis (NST)[1]. The roles of BAT and *UCP1* in energy expenditure and metabolic diseases, such as obesity and type 2 diabetes, have also been extensively investigated[1, 2]. A role for *UCP1* in resistance against obesity was postulated from the results of studies in the genetically modified mice[1, 3, 4] and it is also implicated in the pathogenesis of obesity and metabolic disorders in humans[5-7].

UCP1 is present in most eutherian mammals, but has been lost in both birds and reptiles, and independently lost in several mammalian lineages including the pigs[8]. Loss of *UCP1* in the pig lineage was previously well documented[9,10]. A genetic event eliminating exons 3 to 5 occurred approximately 20 million years ago when the ancestral Suidae were living in tropical and subtropical environments where they could survive without UCP1 mediated NST[10]. The disruption of the *UCP1* gene in pigs consequently resulted in a lack of functional BAT[11]. This evolutionary history has important practical implications for the pig industry. First, modern pigs struggle with poor thermoregulatory abilities, leading to significant neonatal mortality of piglets caused by the cold stress at birth. This is a major welfare issue for the swine industry in cold regions worldwide. Moreover, the involvement of *UCP1* in the pathogenesis of obesity may explain the high levels of fat deposition in pigs. Fat deposition is an economically important trait, influencing pork production, meat quality and dietetic value, as well as growth efficiency[12]. Pig breeding programs have long focused on genetic selection towards less fat deposition and increased leanness which holds great promise for high efficiency pig production[13] .

In theory restoring functional *UCP1* in the domestic pig might enhance the poor thermoregulation and decrease fat deposition to benefit both pig welfare and production. However, it is extremely difficult to create the site specific genome engineering in those mammalian species with no characterized embryonic stem cells available for a classical homologues recombination (HR) targeting strategy. With the recent development of biotechnology, CRISPR/Cas9 system mediated precision genome editing has been reported in mouse[14, 15] which makes knock in, independent of HR, rather than random integration in pigs feasible.

In this study, we generated an adipose tissue specific *UCP1* KI pig model by CRISPR/Cas9 mediated site specific integration, independent of HR. We found that these pigs exhibited significantly

improved thermoregulatory ability. Most strikingly, the ectopic expression of *UCP1* decreased fat deposition without alteration in physical activity and daily energy demands. This highlights the potential of biotechnology applications in pig breeding for improving cold-resistance and lean pork production.

Results

Generation of Adiponectin-UCP1 knock-in pigs

It was previously reported that *UCP1* was disrupted in the pig lineage in a genetic event approximately 20 million years ago[10]. Absence of functional *UCP1* in Bama pigs, a southern Chinese native and cold sensitive breed, was confirmed based on the observation of missing exons 2-5 by protein sequence alignment (Figure S1A) and the undetectable transcriptional expression of *UCP1* in various adipose depots by RT-PCR (Figure S1B).

To insert *UCP1* into the porcine endogenous *UCP* locus, an *UCP1* expression and targeting vector, which contained mouse *UCP1* cDNA driven by adipose tissue specific promoter adiponectin (AdipoQ) and bait sgRNA, was constructed according to a previous report (Figure 1A)[16]. Briefly, the AdipoQ-*UCP1*-3'UTR fragment was sub-cloned into a PLB backbone plasmid, followed by insertion of the bait sequence (labeled in blue: Figure 1A), i.e. the sgRNA target site (capital letters in square frame) and the PAM sequence (lower case letters in square frame) in front of AdipoQ promoter sequence (Figure 1A). The resultant targeting vector provided the donor gene of interest. A Cas9-gRNA plasmid was also constructed as previously demonstrated[17].

The schematic for production of KI pigs is shown as Figure 1B. Firstly, the CRISPR/Cas9 mediated HR independent integration strategy was applied to induce the insertion. In brief, the Cas9-gRNA plasmid and targeting vector were co-transfected into pig embryonic fibroblast cells (PEFs) and then cells were distributed to a 96-well plate by the limited dilution method to obtain single cells in each well. Transfected cells reaching 80% confluence were propagated and genotyped by the primers which were designed to screen the forward integration (P1/P2 for 5'junction, P3/P4 for 3' junction) (Figure 1A). Finally, 3 of 26 cell colonies were identified as positive for forward integration and one of cell colonies (#17) was used to provide donor cells for nuclear transfer (Figure S2, Table S1).

A total of 2553 reconstructed embryos were transferred into the oviducts of 13 recipient surrogates. 3 early pregnancies were established, and all of them went to term. Twelve male piglets

were born by natural delivery (Table S2). Specifically *UCP1* KI was demonstrated by PCR genotyping (Figure 1D) and was further confirmed by the determination of *UCP1* at mRNA (Figure 1E) and protein (Figure 1F) levels in fat depots of the KI pigs. No expression of *UCP1* was observed in other tissues such as the muscle, as expected from the exclusiveness of the adiponectin promoter (Figure 1E).

UCP1 KI pigs exhibited improved thermoregulatory ability

^{18}F-Fluorodeoxyglucose (^{18}F-FDG) Positron Emission Tomography (PET) imaging is routinely used to investigate UCP1 dependent brown adipose tissue (BAT) thermogenesis[18, 19]. To test the ability of *UCP1* KI piglets to cope with a cold environment, 1- month-old WT and KI piglets were housed either at room temperature, or exposed to cold (4°C) for 4 hours and were injected with ^{18}F-FDG through the ear vein. Positive signals from the PET were compared to assess the capacity of ^{18}F-FDG uptake between WT and KI pigs. There were no positive PET signals observed in either WT or KI pigs at room temperature, while the uptake of ^{18}F-FDG was significantly increased in both the abdomen and inguinal subcutaneous fat areas of the KI pigs after cold exposure (Figure 2A).

Next, a time-course cold challenge experiment was conducted with 1-month-old WT and KI piglets (n=6 per group) and the rectal temperatures were monitored and recorded. As shown in Figure 2B, the body temperatures of *UCP1* KI piglets dropped from 39.4 ± 0.16 ℃ to 38.4 ± 0.24 ℃ after 1 hour's cold exposure and then were maintained above 38 °C throughout the 4 hours test period. However, the WT piglets displayed a continued decrease in body temperature within 2 hours' cold exposure, despite the temperatures from 3 h and 4 h were recovered slightly, they were still significantly lower than those from KI (P=0.009 for comparison of 3 h and P=0.04 for 4 h).(Figure 2B). In addition, infrared thermal images of both WT and KI pigs from the ventral side were collected at 0, 2 and 4 h during the cold challenge (Figure S3D). The average surface temperature of three specific areas (labelled 1, 2 and 3) were calculated and the quantification is shown in Figure S3E (n=3 per group). Clearly, significantly improved body temperature maintenance ability was reflected by the higher body temperatures in all the three areas of KI pigs during cold exposure (Figure S3E). The cold challenge experiment was conducted again when these pigs were 6-months-old. Also, higher rectal temperatures in KI pigs were observed compared to that in WT pigs during cold exposure (Figure S3A). Infrared thermal images of ventral (Figure 2C) and dorsal (Figure S3B) sides were collected,

and in agreement with the observations in piglets, KI pigs exhibited higher surface body temperatures just as the quantification data showed (Figure 2D, S3C).

Ectopic-expression of UCP1 enhances mitochondrial function in adipose tissue

UCP1 expression in BAT is tightly correlated with mitochondrial number and/or function. To investigate the effects of ectopic-expression of *UCP1* in porcine adipose tissues on mitochondrial functions, the pre-adipocytes from both WT and KI pigs were successfully cultured and differentiated into mature adipocytes *in vitro* (Figure S4A). Oil-red staining indicated that there were no significant differences in differentiation efficiency (Figure S4A), which was further confirmed by the same expression level of adipogenic marker genes, FABP4 (AP2) and PPARγ, at mRNA and protein levels (Figure S4B and S4C). *UCP1* was exclusively expressed in the adipocytes from KI pigs (Figure S4C). To assess mitochondrial activity, we analyzed the cellular bioenergetics profile using a Seahorse XF24 analyzer (Figure 2E). Our data revealed that despite the similar basal oxygen consumption rate (OCR) in both WT and KI cells (P=0.9927) (Figure 2E, middle panel), the addition of an exogenous uncoupler carbonyl cyanide-4-(trifluoromethoxy) phenylhydrazone (FCCP) increased VO_2 to a higher level in KI cells than in WT cells (P=0.012) (Figure 2E, left panel). As such, UCP1 KI adipocytes displayed significant higher maximal respiration (fold change=1.62, P=0.012) (Figure 2E, right panel), suggesting that ectopic-expression of *UCP1* elevated the spare respiratory capacity of the mitochondria.

Ectopic-expression of UCP1 did not alter physical activity or daily energy expenditure.

Elevated expression of *UCP1* may lead to changes in the overall energy budget linked to greater heat production. If heat production was excessive it might for example lead to reduced physical activity to avoid hyperthermia and alterations in total daily energy expenditure. Physical activity levels were monitored using activity loggers (GT3x) which record movements in three dimensions on a minute by minute timeframe. There was a strong effect of time of day on physical activity levels ($F_{23,161}$=7.96, P<0.001) and a significant random effect of individual nested within genotype ($F_{6,161}$=17.39, P<0.001). However, *UCP1* KI and WT pigs did not differ significantly in their overall physical activity levels (genotype effect $F_{1,161}$=1.74, P=0.189, Figure 2F). The time by genotype interaction was also not significant ($F_{23,144}$=0.3, P=0.99), suggesting the routine heat production by the ectopically expressed UCP1 was not at a level that might cause problems due to the risk of hyperthermia and hence inhibit

activity. We measured daily energy expenditure (DEE) in unconstrained UCP1 KI and WT pigs using the doubly-labelled water method[20]. There was a strong effect of body weight on DEE ($F_{1,9}$=11.23, P=0.009) but no difference between the WT and UCP1 KI animals once the body mass effect had been taken into account using ANCOVA[21] ($F_{1,9}$=0.01, P=0.95) (Figure 2G). The body weight x genotype interaction was not significant ($F_{1,8}$=0.12, P=0.743). Similar results were obtained if the lean tissue mass was used as the predictor variable (lean tissue effect $F_{1,9}$=15.09, P=0.006, genotype $F_{1,9}$=0.13, P=0.729). Fat mass did not explain any of the variation in DEE once the effect of lean mass was accounted for ($F_{1,8}$=0.1, P=0.761).

Decreased fat deposition and increased adipose lipolysis in UCP1 KI pigs

Fat deposition is an important economic trait in pigs, reducing fat deposition has been a major objective in pig breeding programs. Due to the critical role of *UCP1* in energy hemostasis and fat deposition, we were particularly interested in whether *UCP1* expression affected fat deposition in KI pigs. Thus, both WT (n=6) and KI (n=5) pigs were fed *ad libitum* and the body weight was monitored every two weeks until they were 6-months-old. There was no significant difference in body weight between the different genotypes at birth (0.52 ± 0.14 kg for WT vs 0.49 ± 0.06 kg for KI, P=0.63) and 6 months old (27.50 ± 3.23 kg for WT vs 25.67 ± 0.86 kg for KI, P=0.25) (Fig 3A), which indicated the growth rate of KI pigs was not affected. There was also no significant change in the feed conversion ratio during ad libitum feeding in KI pigs (n=5, FCR = 3.12 ± 0.06) compared to those from WT animals (n=6, FCR=3.04 ± 0.13, P=0.59) (Figure 3C), consistent with the absence of an effect on the DEE (above). These pigs (n=6 for WT and n=4 for KI) were slaughtered at 6-month-old and the left carcasses were dissected for further analysis. The detailed slaughter indexes were shown in Table S3. Strikingly, that ratio of lean meat to BMSF weight (sum of bone, muscle, skin and fat weight) from KI pigs was significantly increased by 6.8% (53.12 ± 1.01% of KI vs 49.74 ± 2.43% of WT, P=0.03), while the ratio of fat content to the carcass weight was dramatically decreased by 24.2% (15.28 ± 3.11% of KI vs 20.17 ± 1.80% of WT, P=0.01) compared to those from WT pigs (Figure 3B, Table S3). In agreement with this, significantly thinner back fat was observed in KI pigs: 2.44 mm thinner than WT pigs (6.84 ± 0.45 mm of KI vs 9.28 ± 0.13 mm of WT, P=0.002) (Figure 3D, Table S3).

To investigate why fat accumulation was reduced in *UCP1* KI pigs, fat tissues from different depots of WT and KI pigs, including back, inguinal subcutaneous and peri-renal, were collected and subjected

to haematoxylin and eosin (H&E.) staining and transmission electron microscope (TEM) analysis. It has been demonstrated that activation of *UCP1* in the WAT might promote white adipose tissue browning to prevent diet-induced obesity[22,23]. In the current study, no obvious beige cells were observed in various fat deposition from *UCP1* KI pigs by H&E staining, and the expression levels of beige related genes in WAT were not altered (Figure S3B). However, KI adipocytes from these depots were significantly smaller compared to those from WT pigs (Figure 4A). Further, TEM data showed that many small lipid droplets were found in KI adipocytes, while WT adipocytes contained fewer larger droplets (Figure 4B). However, the mitochondrial copy number was not altered in the inguinal subcutaneous (n = 4 per group, 448.4 ± 71.8 for WT vs 466.8 ± 59.6 for KI, P=0.85) and peri-renal fat (n=4 per group, 985.5 ± 269.2 for WT vs 983.6 ± 70.4 for KI， P=0.99) by QPCR analysis of mitochondrial gene COX2 relative to nuclear gene β-globin (Figure 4D). The presence of small lipid droplets indicated that lipolysis may be enhanced in KI adipocyte. Indeed *in vitro* lipolysis assays showed that under both basal and isoproterenol-stimulated conditions, release of glycerol from inguinal subcutaneous fat explants isolated from *UCP1* KI pigs (n = 4, 0.48 ± 0.08 nmol/mg at basal and 1.2 ± 0.06 nmol/mg after stimulation) was significantly higher by 2 or 1.5 fold than that from WT pigs (n=4, 0.22 ± 0.02 nmol/mg at basal, P=0.02 and 0.75 ± 0.05 nmol/mg after stimulation, P=0.001), respectively (Figure 4C, E). Moreover, the *UCP1* KI pigs showed significantly higher plasma free fatty acid (FFA) levels (n=3 per group, 0.35 ± 0.03 for KI vs 0.21 ± 0.03 for WT, P=0.01) and lower triglycerides (TG) (n=3 per group, 0.18 ± 0.03 for KI vs 0.29 ± 0.01 for WT, P=0.006) without any stimulation (Figure 4G). Further, the expression levels of pHSL and ATGL, two well-recognized lipolysis rate limiting enzymes, were also significantly increased in *UCP1* KI pigs (Figure 4F). Taken together, these data suggested there was increased lipolysis in the *UCP1* KI pigs.

Discussion

Genome editing in pigs is of considerable importance for potential applications in pig production. Recent progress in nuclease mediated genome editing such as the CRISPR/Cas9 technology, provides a precise and highly efficient molecular mechanism for editing cells, tissues and whole organisms[24]. Undoubtedly breeding and trait improvements in livestock will be accelerated by CRISPR-based genome engineering. For example, by deletion of *CD163* with CRISPR/Cas9, pigs have been created that are protected against porcine reproductive and respiratory syndrome virus[25]. Random integration

of a foreign gene into a novel genome often results in unstable phenotypes, gene silencing and unpredictable gene expression patterns, and in some cases, this process is mutagenic[26]. Therefore producing animals carrying exogenous genes integrated at specific genomic loci is far superior[27]. Besides gene disruption, CRISPR/Cas9 also can mediate insertion of exogenous DNA sequences into the specific locus in pigs via HR[28, 29]. However HR is inefficient in many cell types, even a site-specific double-strand break (DSB) is often mediated by nucleases[16]. To overcome the low efficiency of HR mediated knock in, Du et al developed genetic modification in zebrafish genome via non-homologous end joining (NHEJ)[16] which has a much higher efficiency than HR. However until now this strategy has not been tested and reported in pigs.

In this study, combined with somatic cell nuclear transfer, we efficiently inserted adiponectin-*UCP1* into the porcine endogenous *UCP* locus by the application of a CRISPR/Cas9 mediated HR independent approach. During the process of making genetic modifications in the PEFs, 3 of 26 colonies were genotyped as positive for the successful insertion which yielded a KI efficiency of ~11.5 %. Twelve offspring were obtained in three litters and all of them were genotyped to be transgene positive as anticipated. These data indicated that this approach could efficiently insert the foreign fragment as large as 9kb at a specific locus. However junction sequencing analysis revealed some mismatch at both the 5′ and 3′ insertion site suggesting this approach might not suitable for precision insertion.

Adaptive non-shivering thermogenesis generated in BAT enables small eutherian mammals and the neonates of larger animals to maintain high body temperature[30]. Probably because of their tropical evolutionary history, pigs lost functional UCP1 in a genetic event about 20 million years ago. In the current study we confirmed that neither classical BAT, nor detectable *UCP1* gene expression, was observed in neonatal Bama piglets. Correspondingly, it was previously shown that body temperature regulation in the piglet does not rely on BAT-derived non-shivering thermogenesis but is primarily dependent on shivering thermogenesis from skeletal muscle[31]. Previous reports have shown that the newborn piglet usually experiences a sudden and dramatic 15 to 20 °C decrease in its thermal environment, thus the absence of NST makes piglets cold sensitive. Without protection against climatic influences, the piglets would cool down and die and this is a leading cause of neonatal death. This has become a major welfare and economic concern in pig industry[32]. Research in 2008 reported that farmers suffered an average of 20% mortality per litter of piglets[33]. On average, neonatal mortality can

cost farmers 2.56 piglets per litter twice per year, and consequently a farmer with a herd of 250 sows could lose more than €50,000 per year due to early piglet deaths[33]. Neonatal piglet survival has decreased during the last 20 years, but remains a major problem in modern pig production[34].

In small mammals, defective BAT function is strongly associated with increased white fat deposition[35], and in humans increased body mass index is correlated with decreased BAT[36, 37]. Consequently we hypothesized that ectopic expression of *UCP1* in adipocyte tissues may be an attractive approach to enhance the ability of piglets to resist cold and simultaneously decrease fat mass and increase lean meat yield via energy redistribution. Our data confirmed the hypothesis that ectopic expression of *UCP1* in the WAT enhanced the thermogenic capacity of piglets and they were able to maintain their body temperature much better than wild type pigs when faced with actuate exposure to cold (4 ºC). These data are consistent with the observation that *UCP1*-knockout mice are unable to defend their body temperature when acutely exposed to the cold[38]. A potential converse problem of over-expressing UCP1 in white adipose tissue is that the animals might produce too much heat. This would lead to elevated daily energy expenditure, reducing feed conversion ratios, and a risk of hyperthermia. Animals may then attempt to mitigate this hyperthermia risk by reducing their physical activity levels. Hence ectopic expression might succeed only in replacing one economic and welfare issue with a different one. Strikingly, we didn't observe significant changes in the daily energy demands or feed conversion ratios of the UCP1 KI pigs relative to wild types and there was no diminution in physical activity levels of the transgenic pigs. This suggests that the *in* vivo activity of the inserted UCP1 is at a relatively low and safe level with respect to hyperthermia risk.

Mice lacking BAT are susceptible to obesity, whereas mice with increased BAT function, or elevated life span of *UCP1* mRNA are protected against high-fat diet induced obesity[1, 23, 39, 40], suggesting ectopic-expression of *UCP1* may not only improve thermoregulatory status but also have beneficial effects on fatness and carcass traits in the transgenic pigs. The fatness traits are important in pig production since they are related to meat quality and feed efficiency. For a long time, the major objective of pig breeding programs was concentrated on increasing the carcass meat percentage i.e. the lean to fat ratio to improve the feed efficiency (feed-to-gain ratio), as lean growth is much more efficient than the accretion of body fat, and it requires approximately four times the amount of energy to grow one kg of fat tissue as compared to the energy required to grow one kg of lean tissue[13]. Back-fat thickness (BFT) and abdominal fat percentage (AFP) are the most important fatness traits

considered in pig breeding improvement which are negatively correlated to lean percentage[41, 42]. Fat-type pig breeds, including European breeds, such as Mangalica and the Iberian pigs[43], and Chinese breeds, such as the Erhualian, Meishan and Bama pigs[44], produce high-quality meat with desirable palatability attributes, but they have a poor production efficiency such as slow growth rate, poor feed efficiency and carcass composition due to their extreme fatness[45]. For example, previous experiments examining growth performance of Meishan and Yorkshire pigs over a 6-wk period showed that Yorkshire pigs had higher average daily gain (721 vs 353 g/day, respectively, $P<0.01$) and daily feed intake (2.338 vs 1.363 kg/day, respectively, $P<0.01$) and hence greater food conversion efficiency[46]. Researchers also found that pure Meishan pigs had lighter carcass weights, lower lean meat percentages, and higher subcutaneous fat percentages compared with Landrace, Large White, Duroc, and Pietrain pigs[47]. The improvement of fatness traits of these breeds is a necessary step to improving the total efficiency of pork production. Although for commercial pig breeds which are designated 'lean type' breeds, such as the Large White, Landrace and Duroc the fatness traits have been improved greatly by long term selection with a conventional breeding approach, the addition of ractopamine hydrochloride improves their growth performance and carcass characteristics, suggesting that even in 'lean type' commercial pig breeds there is still scope for further improvement in pig fatness traits[48].

Our data confirmed that *UCP1* expression dramatically decreased the AFP (5% less) and BFT (2.54 mm less) in *UCP1* KI pigs, which was consistent with previous reports that overexpression *UCP1* in WAT results in decreased fat deposition in mice[1, 49]. Besides that, the lean meat rate was increased significantly as a result of lower fat accumulation. Notably, unlike IGF1 transgenic pigs, which had markedly reduced fat deposition and significant growth enhancement, but at the expense of problems such as fatigue, gastric ulcers, and low libido (although fertile) compared to WT pigs[50], our *UCP1* transgenic pigs had a normal growth rate, were healthy, showed normal activity levels and didn't show any obvious defects of behavior. The molecular basis of the improved fat traits appeared to be a result of increased lipolysis in the white adipose tissue as evidenced by the smaller lipid droplet in WAT, up-regulated expression of lipolysis proteins, and significant higher FFA and lower TG in plasma. These results are consistent with the studies that disruption of *UCP1* in mice could completely impair lipolysis[51, 52].

In summary, *UCP1* transgenic pigs were generated by site-specific KI strategy and were both cold tolerant as piglets and had improved carcass quality as adults. Development of this pig model is

not only valuable for alleviation of a major economic and welfare issue but also leads to the improvement of economic important pig meat traits.

Material and Methods

Ethics statement and animal housing

All experiments involving animals were conducted according to the Guidelines for the Care and Use of Laboratory Animals established by the Beijing Association for Laboratory Animal Science and approved by the Animal Ethics Committee of Institute of Zoology, Chinese Academy of Sciences, China. Pigs were raised at the Beijing Farm Animal Research Center. Feed was given twice daily till 2 month old when the pigs were fed ad libitum. The pigs and feed were weighed at 1 month interval to calculate average daily gain (ADG) and feed efficiency.

Plasmids

For construction of targeting vector, AdipoQ-UCP1-3'UTR fragment was first digested from pcDNA3.1 and then cloned to the PLB vector using lethal based fast cloning kit (Tiangen Biotech, Beijing, China). The resulting plasmid was linearized by BspEI (New England Biolabs, MA, USA) digestion. Finally, the bait sequence was inserted into the linearized plasmid to constitute the donor vector. The CRISPR/Cas9 construct was obtained as previously described (ref).

Cell culture and transfection

Primary pig embryonic fibroblast (PEF) cells were isolated as previously reported. Cas9-gRNA plasmid were co-transfected to the cultured PEF cells with the nucleofection method. Forty-eight hours after the transfection, cells were harvested using 0.25 % trypsin/EDTA (Gibco, NY, USA), and the cell density was calculated using handheld automated cell counter (Millpore, MA, USA). Single cell was plated in each well of 96-well plates by limited dilution and cultured for approximately 10 days in cell culture medium supplemented with 2.5 ng/mL basic fibroblast growth factor (Sigma, MO, USA). The medium was replaced every 4 days. Confluent cell colonies were propagated and genotyped by PCR and sequencing.

Nuclear transfer and embryo transfer

Pig ovaries were collected from a local slaughterhouse and transported to the laboratory within 1 h in 0.9% saline maintained at 37℃. In vitro maturation of oocytes, enucleation, microinjection, and fusion of reconstructed oocytes were carried out in our laboratory according to previously described methods. The reconstructed embryos were cultured in porcine zygote medium (PZM3) in 5% CO^2 at 39 °C for 14-16 h until embryo transfer. Embryos in good condition were surgically transferred into the oviduct of a surrogate the day after observed estrus. Gestation was detected by ultrasound at day 28 after embryo transfer. All of the cloned piglets were delivered by natural birth.

PET

Data were acquired for all studies in this work using a whole-body PET scanner (Judicious PET L900), which was developed by the Institute of High Energy Physics, Chinese Academy of Sciences. The scanner uses LYSO-based detector blocks with a 70 cm transaxial field-of-view (FOV) and a 21.6 cm axial FOV. According to the National Electrical Manufacturers Association (NEMA) NU 2-2007 procedures, the transverse (axial) spatial resolution FWHMs were measured to be 4.4 (3.9) mm and 5.1 (4.0) mm at 1 and 10 cm off axis, respectively, and the sensitivity average at 0 and 10 cm was 13.2 cps/kBq. The emission projection data were acquired in listmode format and were Fourier re-binned into two-dimensional (2D) sinograms. Images were then reconstructed using the 2D OSEM algorithm (four iterations and sixteen subsets), resulting in 2.0×2.0×1.8 mm3 voxel size for a 320×320×119 image volume. The PET images were corrected for detector efficiency, dead-time, decay, photon scatter and attenuation.

Cold challenge experiment

1-month-old piglets and 6-month-old pigs were subjected to cold stimulation. Pigs at 1-month-old age were placed in a cold chamber (4 °C) for up to 4 hours and pigs of 6-month-old were kept in separate cages in the open air since the air temperature reached nearly 0 °C at that time. Rectal temperatures of pigs were measured using a rectal probe connected to a digital thermometer (Jinming Instrument Co. Ltd., Tianjin, China) every 1 hour. Infrared pictures were taken by infrared camera (FLIR Systems, Inc. USA). Photos were processed and temperatures quantified using FLIR Tools software.

Porcine primary pre-adipocyte isolation and in vitro differentiation

Adipose tissues were harvested from two-week-old piglets, minced and digested with 2 mg/ml

collagenase type I (Sigma, MO, USA) in DMEM/F12 plus 1% fatty-acid-free bovine serum albumin (BSA) (Sigma, MO, USA) for 60 min at 37°C. SVF cells were collected with a cell strainer (70μm diameter) and then plated and grown in DMEM/F12 (Gibco, NY, USA) supplemented with 10% fetal bovine serum (FBS) (Sigma, MO, USA) and 1% penicillin-streptomycin. For white adipocyte differentiation, cells were grown until confluence and then were treated with human WAT induction medium (DMEM/H medium containing 0.25 mM isobutylmethylxanthine, 0.1 μM dexamethasone, 66 nm human insulin (Sigma, MO, USA), 17 μM pantothenate, 33 μM biotin, 20 mM HEPES (pH 7.4) and 0.5% FBS) for 5 days. At day 5, half of the induction medium was removed, and the same volume of human WAT mature medium (DMEM/H medium containing 0.1 μM dexamethasone, 66 nm human insulin, 17 μM pantothenate, 33 μM biotin, 20 mM HEPES (pH 7.4) and 10% FBS) was added. One day after, the cells were cultured in pure human WAT maturation medium for 2 d. On day 8, the fully differentiated adipocytes were used for all the following experiments.

Bioenergetic profiling

Pig primary subcutaneous adipocytes were seeded into gelatin-coated XF24 culture microplates (Seahorse Bioscience, CA, USA) and cultured in DMEM/F12 with 10% FBS and antibiotics (100units/mL of penicillin and 100μg/mL of streptomycin) overnight at 37 °C in an atmosphere of 5% CO_2. Next day, the cells were cultured in differentiation medium. On day 8, the O2 consumption was measured with a Seahorse Bioscience XF24-3 extracellular flux analyzer. To measure OCR independent of oxidative phosphorylation, 1 μM oligomycin was added to cells. Subsequently, 0.5 μM FCCP (carbonyl cyanide-p-trifluoromethoxyphenylhydrazone) and 2 μM respiratory chain inhibitor (rotenone) were added to measure the maximal respiration and basal non-mitochondrial respiration rates. The means and standard error of the mean (s.e.m.) from three independent experiments are shown. Statistical comparisons were made using Student's t-test.

Physical activity measurement

When pigs reached 2 month old, they were divided into separate pens to measure their physical activity levels. Actigraph GT3x activity monitors on collars were attached to the necks of the pigs to perform the measurement. The activity logger measures the activity in three axes using accelerometers. Axis X measures acceleration in forward/backward motions, axis Y measures sideways and axis Z measures

up/down motions. The units of measurement are counts integrated across all 3 dimensions and which reflects the activity intensity of animals (called the vector magnitude). The values were recorded for 4 KI and 4 WT pigs at 1 minute interval and the measurement lasted continuously for 5 days. The data were averaged over each hour and across the sample of KI and WT animals. Data were analysed using ANOVA with time of day and genotype as factors. Individual was included as a random factor nested within time in the analysis to account for repeated measurements.

Doubly-labelled water

Daily energy expenditure (DEE, kJ/day) was measured using the doubly labelled water (DLW) technique (Lifson & McClintock 1966; Butler et al 2004) in a total of 12 pigs (6 KI and 6 WT). This method has been previously validated on multiple occasions by comparison to simultaneous indirect calorimetry in large animals such as humans and provides an estimate of energy expenditure with a precision of better than 6% (reviewed in Speakman 1997). On day one, the animals were weighed (±100 g) and a 100 uL blood sample was obtained to estimate the background isotope enrichments of ^{2}H and ^{18}O (Speakman and Racey, 1987 - method D). Blood samples were immediately heat sealed into 2 x 100µL glass capillaries, which were stored at room temperature. Afterwards, a known mass of DLW (660000 ppm ^{18}O, 328000 ppm ^{2}H was administered intraperitoneally). Syringes were weighed before and after administration (± 0.001g, Sartorius balance) to calculate the exact mass of DLW injected. Blood samples were taken after one, two and three hours of isotope equilibration to estimate initial isotope enrichments (Krol and Speakman, 1999). Subsequent samples were collected daily as close to multiples of 24h as possible to avoid circadian effects (Speakman and Racey, 1988). Animals were measured over 5 days. Making measurements across multiple days minimizes the large day to day variability in DEE (Speakman et al, 1994). Analysis of the isotopic enrichment of blood was performed blind of the animal genotype, using a Liquid Isotope Water Analyser (Los Gatos Research, USA) (Berman et al, 2013). Initially the blood was vacuum distilled (Nagy, 1983), and the resulting distillate was used for analysis. Samples were run alongside five lab standards for each isotope and International standards to correct delta values to ppm. Daily isotope enrichments were $\log_e$ converted and the elimination constants (k_o and k_d) were calculated by fitting a least squares regression model to the $\log_e$ converted data. The back extrapolated intercept was used to calculate the isotope dilution spaces (N_o and N_d). These pigs have a body mass that sits in the region where it is not entirely clear from validation studies

whether a two-pool or a single pool model should be used to calculate the CO_2 production and hence energy expenditure. Data presented in the paper refer to calculations using a two-pool model, specifically equation A6 from Schoeller et al (1986) as recommended by Speakman (1993) for animals weighing > 5kg. We also calculated the data using a single pool model (equation 7.17 from Speakman 1997) to confirm that the outcomes were not affected by the choice of model as recommended by Speakman and Hambly (2016).

Quantitative PCR analysis

Total RNA was isolated from pig adipose tissue with TRIzol (Invitrogen) extraction. First-strand complementary DNA synthesis was performed using the FastQuant RT Kit (Tiangen Biotech, Beijing, China). Quantitative real-time PCR reaction were performed using the SYBR Premix Ex Taq (Tli RNaseH Plus) (Takara) on an Agilent Mx3005p (Agilent Technologies, CA, USA) with reaction volumes of 20 ml. The primer sequences are listed in Supplementary Table S4. Relative gene expression was calculated using the comparative cycle threshold (2^{-ddCt}) method. Statistical analysis was performed with GraphPad Prism 6.0.

Western blotting

Fat tissues were dissected, frozen immediately in liquid nitrogen and stored at -80°C until use. Total proteins from tissue or cultured adipocyte were extracted using Minute Total Protein Extraction Kit (Invent Biotechnologies, Inc. MN, USA). The proteins were subjected to western blot analysis with the following desired antibodies: anti-UCP1 for tissues (GTX632673, 1:1000, GeneTex, Inc. CA, USA), anti-UCP1 for adipocytes (ab10983, 1:1000, Abcam, MA, USA), anti-ATGL (2439, 1:2000, CST, MA, USA), anti-HSL (4107, 1:2000, CST, MA, USA), anti-pHSL (4139 for Ser563, 4126 for Ser660, 1:2000, CST, MA, USA), anti-PPARG (ab45036, 1:2000, Abcam, MA, USA), anti-Tubulin (sc-9104, 1:3000, Santa Cruz Biotech, CA, USA). The blots were developed using HRP-conjugated secondary antibodies and the ECL-plus system. All signals were visualized and analyzed with Tanon 5200 (Tanon Science & Technology Co. Ltd., Shanghai, China).

Microscopy

Adipose tissues were excised and fixed in 4% paraformaldehyde, dehydrated overnight in 70% ethanol. The fixed specimens were processed to paraffin blocks, sectioned and stained with haematoxylin-eosin

using a standard protocol. Fat cell size was measured using ImageJ software. For transmission electron microscopy, adipose tissues sections were fixed in 2% (vol/vol) glutaraldehyde in 100 mM phosphate buffer, pH 7.2, for 12 h at 4 °C. The samples were then post-fixed in 1% osmium tetroxide, dehydrated in ascending gradations of ethanol and embedded in fresh epoxy resin 618. Ultra-thin sections (60-80 nm) were cut and stained with lead citrate before being examined on a Phillip CM-120 transmission electron microscope.

Ex Vivo Lipolysis Measurement

For ex vivo lipolysis, subcutaneous and perirenal fat pads (~0.5 g) isolated from pig were incubated at 37 °C in 1.0 mL phenol red–free Dulbecco's modified Eagle's medium containing 2% FA-free BSA with or without 1 μmol/L isoproterenol. The contents of glycerol (BioAssay Systems, EAPL-200) in incubation media were quantified according to the manufacturer's protocols.

Blood Lipid Analysis

After collection of blood samples, serum from each pig was prepared and stored at -80℃ until use. Total serum levels of cholesterol, TG, FFA, Low-density lipoprotein-cholesterol (LDL-C), and high-density lipoprotein cholesterol (HDL-C) were measured in the 306th hospital of PLA (Beijing, China).

Carcass trait measurements

The pigs were fasted for 24h before slaughter and anaesthetized to death. At slaughter, the carcass was split longitudinally and the head, hair, feet, viscera (expect for leaf fat and kidney) were removed. Carcass weight (CW) was recorded. The dressing percentage for an individual animal was defined as CW divided by the live weight. Measurements of backfat depth at the midline were conducted with a vernier caliper at the scapular margin, the last rib and the lumbosacral junction respectively and the average backfat thickness of the three points was adopted. Measurements of the longissimus muscle area (LMA) was conducted on the cut surface at the intercostal space between the 10th and 11th ribs by planimeter . As the backfat was strongly correlated to the body weight, all the measured data of backfat was revised to that of 20 kg body weight according to the regression equation established in our own farm: bf = 6.218 + 0.2125w (R^2=0.7884), bf and w represents backfat and body weight respectively. The left carcass was dissected to lean meat, fat, skin and bone. The percentage of each

part was calculated by dividing each by sum weight of the four parts.

Statistical Analysis

The statistical data reported includes results from at least three biological replicates. All results are expressed as mean ± s.e.m. For normal distribution data, differences between two groups were assessed by unpaired Student's t test.

Acknowledgement

We are grateful to members of Zhao, Jin and Wang laboratories for helpful discussions, to P. Chai, S. Liu, H. Tang, and C. Wei from the Institute of High Energy Physics at the Chinese Academy of Sciences and Beijing Engineering Research Center of Radiographic Techniques and Equipment for their great help with the PET scan experiments and analysis, and to Peter Thomson at the University of Aberdeen for technical assistance with isotope analysis This study was supported by the National Transgenic Project of China (2016ZX08009003-006-007), the Strategic Priority Research Programs of CAS (XDA08010304 and XDB13030000) and the Agricultural Science and Technology Innovation program (ASTIP-IAS05). Y. Wang was supported by the Elite Youth Program of the Chinese Academy of Agricultural Sciences.

References

1. Kopecky, J., Clarke, G., Enerback, S., Spiegelman, B. & Kozak, L.P. Expression of the mitochondrial uncoupling protein gene from the aP2 gene promoter prevents genetic obesity. *The Journal of clinical investigation* **96**, 2914-2923 (1995).
2. Wang, W. & Seale, P. Control of brown and beige fat development. *Nature reviews. Molecular cell biology* **17**, 691-702 (2016).
3. Li, B. et al. Skeletal muscle respiratory uncoupling prevents diet-induced obesity and insulin resistance in mice. *Nature medicine* **6**, 1115-1120 (2000).
4. Lowell, B.B. et al. Development of obesity in transgenic mice after genetic ablation of brown adipose tissue. *Nature* **366**, 740-742 (1993).
5. Garruti, G. & Ricquier, D. Analysis of uncoupling protein and its mRNA in adipose tissue deposits of adult

humans. *International journal of obesity and related metabolic disorders : journal of the International Association for the Study of Obesity* **16**, 383-390 (1992).

6. Lowell, B.B. & Flier, J.S. Brown adipose tissue, beta 3-adrenergic receptors, and obesity. *Annual review of medicine* **48**, 307-316 (1997).
7. Villarroya, F., Cereijo, R., Villarroya, J. & Giralt, M. Brown adipose tissue as a secretory organ. *Nature reviews. Endocrinology* (2016).
8. McGaugh, S. & Schwartz, T.S. Here and there, but not everywhere: repeated loss of uncoupling protein 1 in amniotes. *Biology letters* **13** (2017).
9. Trayhurn, P., Temple, N.J. & Van Aerde, J. Evidence from immunoblotting studies on uncoupling protein that brown adipose tissue is not present in the domestic pig. *Canadian journal of physiology and pharmacology* **67**, 1480-1485 (1989).
10. Berg, F., Gustafson, U. & Andersson, L. The uncoupling protein 1 gene (UCP1) is disrupted in the pig lineage: a genetic explanation for poor thermoregulation in piglets. *PLoS genetics* **2**, e129 (2006).
11. Jastroch, M. & Andersson, L. When pigs fly, UCP1 makes heat. *Molecular metabolism* **4**, 359-362 (2015).
12. Wood, J.D. et al. Fat deposition, fatty acid composition and meat quality: A review. *Meat science* **78**, 343-358 (2008).
13. Patience, J.F., Rossoni-Serao, M.C. & Gutierrez, N.A. A review of feed efficiency in swine: biology and application. *J Anim Sci Biotechnol* **6**, 33 (2015).
14. Cong, L. et al. Multiplex genome engineering using CRISPR/Cas systems. *Science* **339**, 819-823 (2013).
15. Hai, T., Teng, F., Guo, R., Li, W. & Zhou, Q. One-step generation of knockout pigs by zygote injection of CRISPR/Cas system. *Cell research* **24**, 372-375 (2014).
16. Li, J. et al. Intron targeting-mediated and endogenous gene integrity-maintaining knockin in zebrafish using the CRISPR/Cas9 system. *Cell research* **25**, 634-637 (2015).
17. Wang, X. et al. One-step generation of triple gene-targeted pigs using CRISPR/Cas9 system. *Scientific reports* **6**, 20620 (2016).
18. Virtanen, K.A. et al. Functional brown adipose tissue in healthy adults. *The New England journal of medicine* **360**, 1518-1525 (2009).
19. Cypess, A.M. et al. Identification and importance of brown adipose tissue in adult humans. *The New England journal of medicine* **360**, 1509-1517 (2009).
20. Butler, P.J., Green, J.A., Boyd, I.L. & Speakman, J.R. Measuring metabolic rate in the field: the pros and cons of the doubly labelled water and heart rate methods. *Functional Ecology* **18**, 168-183 (2004).
21. Tschop, M.H. et al. A guide to analysis of mouse energy metabolism. *Nature methods* **9**, 57-63 (2011).
22. Schulz, T.J. & Tseng, Y.H. Brown adipose tissue: development, metabolism and beyond. *The Biochemical journal* **453**, 167-178 (2013).
23. Dempersmier, J. et al. Cold-inducible Zfp516 activates UCP1 transcription to promote browning of white fat and development of brown fat. *Molecular cell* **57**, 235-246 (2015).
24. Barrangou, R. & Doudna, J.A. Applications of CRISPR technologies in research and beyond. *Nature biotechnology* **34**, 933-941 (2016).
25. Whitworth, K.M. et al. Gene-edited pigs are protected from porcine reproductive and respiratory syndrome virus. *Nature biotechnology* **34**, 20-22 (2016).
26. Ruan, J. et al. Highly efficient CRISPR/Cas9-mediated transgene knockin at the H11 locus in pigs. *Scientific reports* **5**, 14253 (2015).
27. Capecchi, M.R. Gene targeting in mice: functional analysis of the mammalian genome for the twenty-first century. *Nature reviews. Genetics* **6**, 507-512 (2005).

28. Peng, J. et al. Production of Human Albumin in Pigs Through CRISPR/Cas9-Mediated Knockin of Human cDNA into Swine Albumin Locus in the Zygotes. *Scientific reports* **5**, 16705 (2015).
29. Lai, S. et al. Generation of Knock-In Pigs Carrying Oct4-tdTomato Reporter through CRISPR/Cas9-Mediated Genome Engineering. *PloS one* **11**, e0146562 (2016).
30. Cannon, B. & Nedergaard, J. Brown adipose tissue: function and physiological significance. *Physiological reviews* **84**, 277-359 (2004).
31. Symonds, M.E. & Lomax, M.A. Maternal and environmental influences on thermoregulation in the neonate. *The Proceedings of the Nutrition Society* **51**, 165-172 (1992).
32. Wischner, D., Kemper, N. & Krieter, J. Nest-building behaviour in sows and consequences for pig husbandry. *Livestock Science* **124**, 1-8 (2009).
33. Project, W.Q. in ScienceDaily (September 4, 2008).
34. Theil, P.K., Lauridsen, C. & Quesnel, H. Neonatal piglet survival: impact of sow nutrition around parturition on fetal glycogen deposition and production and composition of colostrum and transient milk. *Animal* **8**, 1021-1030 (2014).
35. Hamann, A., Flier, J.S. & Lowell, B.B. Decreased brown fat markedly enhances susceptibility to diet-induced obesity, diabetes, and hyperlipidemia. *Endocrinology* **137**, 21-29 (1996).
36. Vijgen, G.H. et al. Increase in brown adipose tissue activity after weight loss in morbidly obese subjects. *The Journal of clinical endocrinology and metabolism* **97**, E1229-1233 (2012).
37. Vijgen, G.H. et al. Brown adipose tissue in morbidly obese subjects. *PloS one* **6**, e17247 (2011).
38. Enerback, S. et al. Mice lacking mitochondrial uncoupling protein are cold-sensitive but not obese. *Nature* **387**, 90-94 (1997).
39. Qiang, L. et al. Brown remodeling of white adipose tissue by SirT1-dependent deacetylation of Ppargamma. *Cell* **150**, 620-632 (2012).
40. Takahashi, A. et al. Post-transcriptional Stabilization of Ucp1 mRNA Protects Mice from Diet-Induced Obesity. *Cell reports* **13**, 2756-2767 (2015).
41. Knecht, D. & Duziński, K. The effect of sex, carcass mass, back fat thickness and lean meat content on pork ham and loin characteristics. *Arch. Anim. Breed.* **59**, 51-57 (2016).
42. Jacyno, E., Pietruszka, A., Kaw cka, M., Biel, W. & Kotodziej-Skalska, A. Phenotypic correlations of backfat thickness with meatiness traits, intramuscular fat, longissimus muscle cholesterol and fatty acid composition in pigs. *South African Journal of Animal Science* **45**, 122-128 (2015).
43. Lopez-Bote, C.J. Sustained utilization of the Iberian pig breed. *Meat science* **49S1**, S17-27 (1998).
44. Ai, H. et al. Detection of quantitative trait loci for growth- and fatness-related traits in a large-scale White Duroc x Erhualian intercross pig population. *Animal genetics* **43**, 383-391 (2012).
45. Jiang, Y.Z. et al. Carcass and meat quality traits of four commercial pig crossbreeds in China. *Genetics and molecular research : GMR* **11**, 4447-4455 (2012).
46. Hyun, Y., Wolter, B.F. & Ellis, M. Feed intake patterns and growth performance of purebred and crossbred Meishan and Yorkshire pigs. *Asian Australasian Journal of Animal Sciences* **14**, 837-843 (2001).
47. Gispert, M. et al. Relationships between carcass quality parameters and genetic types. *Meat science* **77**, 397-404 (2007).
48. Lowe, B.K. et al. Effects of feeding ractopamine hydrochloride (Paylean) to physical and immunological castrates (Improvest) in a commercial setting on carcass cutting yields and loin quality. *Journal of animal science* **92**, 3715-3726 (2014).
49. Rossmeisl, M. et al. Expression of the uncoupling protein 1 from the aP2 gene promoter stimulates mitochondrial biogenesis in unilocular adipocytes in vivo. *European journal of biochemistry* **269**, 19-28 (2002).

50. Pursel, V.G. et al. Expression and performance in transgenic pigs. *J Reprod Fertil Suppl* **40**, 235-245 (1990).
51. Dong, M. et al. Cold exposure promotes atherosclerotic plaque growth and instability via UCP1-dependent lipolysis. *Cell metabolism* **18**, 118-129 (2013).
52. Mottillo, E.P. et al. Coupling of lipolysis and de novo lipogenesis in brown, beige, and white adipose tissues during chronic beta3-adrenergic receptor activation. *Journal of lipid research* **55**, 2276-2286 (2014).

Figure legends

Figure 1. CRISPR/Cas9 mediated HDR independent integration efficiently produce Adiponectin-UCP1 knock in pigs.

(A) Schematic representation of the design of targeting vector. Exons of *UCP1* are shown as purple red boxes and cyan box in exon 2 represents sgRNA targeting site, which is enlarged to a rectangle box with PAM sequence labeled in lower case letter and targeting sequence in capital letter in it. Cyan box in the targeting vector is the same as the one in exon 2, which is also called bait sequence. Red and yellow boxes representing AdipoQ promoter and 3'UTR constitute the promoter element, and *UCP1* in green locates in the middle. Forward integration happens if 5' site at the DSB of targeting vector is ligated behind 3' site of the DSB in *UCP1* locus. Four pair of primers are designed for genotyping. P1/P2 and P3/P4 are designed for genotyping 5' junction and 3' junction in the transgenic colonies, respectively. P5/P6 and F/R primers are designed for detecting donor vector region and undamaged genomic sequence in the cloned pigs, respectively. (B) Schematic overview of production of KI pigs. (C) KI pigs at day 15. (D) PCR genotyping confirmed site-specific insertion of donor DNA in the cloned pigs. Lane 1-12 represents12 individuals; Lane N1, N2 represent two negative control of wild type pigs. RT-PCR analysis of *UCP1* from WT and KI adipose determined the expression of the foreign gene. Back sub represents back subcutaneous fat; Inguinal sub represents inguinal subcutaneous fat. (E) Western blot analysis confirmed the *UCP1* expression in the KI pigs (n=3).

Figure 2. Ectopic-expression of UCP1 improves thermoregulation capacity in pigs.

(A) Positron Emission Tomography (PET) analysis of 1-month-old WT and KI piglets at room temperature (RT) or after cold stimulation (Cold). Positive signals were identified in KI pigs after cold exposure indicated by white arrows. (B) Rectal temperature monitor of 1-month-old WT (n=6) and KI (n=6) piglets during cold stimulation for 4 hour revealed KI pigs were more tolerant to cold challenge. (C) Infrared pictures were taken at 0, 2, 4 hour after cold exposure in 6-month-old pigs. White-dotted line depicts areas labelled 1, 2, 3 of where temperatures are to be quantified. Higher temperature could be seen in KI pigs from the thermal picture (D) Temperature quantification of area 1, 2, 3 between WT and KI (n=4 per group) pigs at different time points. Aver-temp represents average temperature. (E) Oxygen consumption rate (OCR) in differentiated white adipocytes from WT and KI pigs showed similar basal cellular respiration but higher maximal respiration in KI cells. (F) Physical activity levels

(vector magnitude counts) using the GT3x accelerometer in live pigs as a function of time of day. Red points are UCP1 KI transgenic pigs (n=4) and blue points are WT controls (n=4). There was no effect of genotype on physical activity levels. (G) Daily energy expenditure (MJ/day) by DLW on free-roaming pigs in relation to body weight. Red points and red line (fitted regression) are UCP1 KI transgenic pigs (n=6) and blue points and blue line are WT controls (n=6). There was a strong effect of body weight but no effect of genotype on DEE. Values are shown as the mean ± standard error of the mean (s.e.m.), significant differences compared with controls are indicated by $**P < 0.01$, $*P < 0.05$; data were analyzed with a two-sample t-test. In F and G the data were analysed by general linear models.

Figure 3. Ectopic-expression of UCP1 decreases fat deposition in pigs.

(A) Growth curve from birth to 6 month old showing no difference in body weight between WT (n=6) and KI (n = 5) pigs. A growth spurt happens at 2.5 month old because of the start of ad libitum feed at this time. (B) There is no difference of feed conversion ratio between WT (n = 6) and KI (n = 5) pigs during the ad libitum feed period. (C) The proportion of carcass to body weight (dressing percentage), lean meat and fat to BMSF weight (sum weight of bone, muscle, skin and fat dissected from left half carcass) between WT (n = 6) and KI (n = 4) pigs. Dressing percentage showed no difference but higher lean meat percentage and lower fat percentage were found in KI pigs. (D) Backfat revised to that of 20 kg body weight in KI pigs (n = 4) is significantly thinner than that of WT pigs (n = 4). Values are shown as the mean ± s.e.m., significant differences compared with controls are indicated by $**P < 0.01$, $*P < 0.05$; data were analyzed with a two-sample t-test.

Figure 4. Ectopic-expression of UCP1 promotes lipolysis.

(A) Haematoxylin and eosin (H&E.) staining of adipocyte from backfat (upper panel), inguinal sub fat (middle panel) and perirenal fat (lower panel) depicted smaller fat cell in KI pigs. Scale bar represents 50 μm. (B) The distribution of fat cell size from the three fat depot between WT and KI pigs. At least 200 fat cells were counted in each genotype. (C) Transmission electron microscope analysis of adipocyte from backfat (upper panel), inguinal sub fat (middle panel) and perirenal fat (lower panel). Small lipid droplets indicated by red arrows were identified in KI adipocytes. Scale bar represents 5 μm. (D) Relative mitochondria (mt) copy number analysis of inguinal sub fat and perirenal fat showed

no difference between the two genotypes (n = 4 per group). (E) Measurement of glycerol release in inguinal sub fat at 1.5h and 3h showed higher content in KI pigs either at basal level or after ISO stimulation (n = 4 per group). (F) Western blot analysis showed higher expression levels of ATGL, pHSL and HSL protein in KI inguinal sub fat compared to WT (n = 3 per group). (G) Serum concentration of TG was significantly decreased but increased of FFA in KI pigs (n = 3 per group). Values are shown as the mean ± s.e.m., significant differences compared with controls are indicated by $**P < 0.01$, $*P < 0.05$; data were analyzed with a two-sample t-test.

Figure S1. UCP1 lacks exon 3-5 and can't be detected in fat depot from Bama pig at postnatal day 15 and 30. (A) Alignment of UCP1 protein sequences of human, mouse, bovine, Yorkshire and Bama pig. Black arrows marks the end of each exon of human sequence. Red arrows indicate SNPs between Yorkshire and Bama pigs. (B) Transcription of UCP1 was not detected from wild type pigs at postnatal day 15 and 30 by semi-quantitative-PCR. UCP1-1 represents a 106 bp product across exon 1-2, and UCP1-2 represents a 142 bp product across exon 2-3 of UCP1. Rip140 is used as a positive control and Cyclophilin A (CycloA), an internal control.

Figure S2. Homology-independent integration is an efficient tool to create insertion. (A) Genotyping of the 26 cell clones. P1/P2 and P3/P4 are two primers to detect 5′ junction and 3′ junction. Cell clones with bands at both P1/P2 and P3/P4 are possibly transgenic, which are marked by white arrows. M represents marker; N represents negative wild type cell; P represents positive plasmid with two homology arms amplified from genome UCP1 sequence flanking Adiponectin-UCP1-3'UTR, as a result, P1/P2 can be detected from the positive plasmid, but P3/P4 can't. (B) Sanger sequencing of 5' junction and 3' junction confirming the targeted insertion of exogenous DNA.

Figure S3. Thermoregulation was improved after UCP1 overexpression. (A) Rectal temperature monitoring of WT and KI (n=6 per group) pigs at their age of 6 months during 4 hour' cold stimulation. (B) Infrared pictures from dorsal side of 6-month-old pigs taken at 0, 2, 4 hour after cold exposure. White-dotted line depicts area labeled A whose temperature is to be quantified. (C) Quantification of area A between WT and KI (n=4 per group) pigs at different time points. (D) Infrared pictures from ventral side of 1 month old pigs taken at 0, 2, 4 hour after cold exposure. White-dotted line depicts

areas labeled 1, 2, 3 whose temperatures are to be quantified. (E) Quantification of area 1, 2, 3 between WT and KI (n=3 per group) pigs at different time points. Aver-temp represents average temperature. Values are shown as the mean ± s.e.m., significant differences compared with controls are indicated by $**P< 0.01$, $*P< 0.05$; data were analyzed with a two-sample t-test.

Figure S4. UCP1 overexpression does not affect white adipocyte differentiation. (A) Representative Oil-Red-O staining of differentiated white adipocyte. (B) Relative mRNA expression level of marker genes of differentiated white adipocyte, AP2 and PPARG between WT and KI (n=4 per group). (C) Protein expression level of *Pparγ* and *Ucp1* between WT and KI (n=3 per group) differentiated white adipocytes.

Figure S5. UCP1 overexpression did not induce WAT browning. (A-D) Relative mRNA expression level of WAT browning markers from backfat (A), inguinal sub fat (B), leaf fat (C), and perirenal fat (D).

Supplementary references for DLW section:

Berman, E., Fortson, S., Snaith, S., Gupta, M., Chery, I., Blanc, S., Melanson, E., Thomson, P., and Speakman, J.R. (2013) Direct analysis of δ2H and δ18O in natural and enriched human urine using laser-based, Off-Axis Integrated Cavity Output Spectroscopy. Analytical Chemistry 84: 9768-9773.

Butler, P.J., Green, J.A., Boyd, I.L. and Speakman, J.R. (2004) Measuring metabolic rate in the field: the pros and cons of the doubly-labelled water and heart rate methods Functional Ecology 18: 168-183.

Krol, E. and Speakman, J.R. (1999) Isotope dilution spaces of mice injected simultaneously with deuterium, tritium and oxygen-18. Journal of Experimental Biology 202:2839-2849.

Nagy, K.A. (1983) The Doubly Labeled Water (3HH18O) Method: a guide to its use. UCLA Publication no 12-1417, UCLA, Los Angeles, CA.

Schoeller, D. A., Ravussin, E., Schutz, Y., Acheson, K. J., Baertschi, P. and Jéquier, E. (1986). Energy expenditure by doubly labeled water: validation in humans and proposed calculation. Am. J. Physiol. 250, R823-R830.

Speakman, J.R. and Hambly, C. (2016) Using doubly-labeled water to measure free-living energy expenditure: some old things to remember and some new things to consider. Comp. Biochem. Physiol. 202: 3-9.

Speakman, J.R. and Racey, P.A. (1987) The equilibrium concentration of O-18 in body-water – implications for the accuracy of the doubly-labeled water technique and a potential new method of measuring RQ in free-living animals. Journal of Theoretical Biology 127: 79-95.

Speakman, J.R. and Racey, P.A. (1988) Consequences of non-steady state CO2 production for

accuracy of the doubly-labeled water technique – the importance of recapture interval. Comp Biochem. Physiol. A 90: 337-340.
Speakman, J.R., Racey, P.A., Haim, A., Webb, P.I., Ellison, G.T.H., and Skinner, J.D. (1994) Interindividual and intraindividual variation in daily energy expenditure of the pouched mouse (Saccostomus campestris). Functional Ecol. 8: 336-342.
Speakman, J.R. (1993) How should we calculate CO2 production in doubly labeled water studies of animals? Functional Ecol. 7, 746–750.
Speakman, J.R. (1997) Doubly-labelled water: theory and practice. Chapman and Hall London.

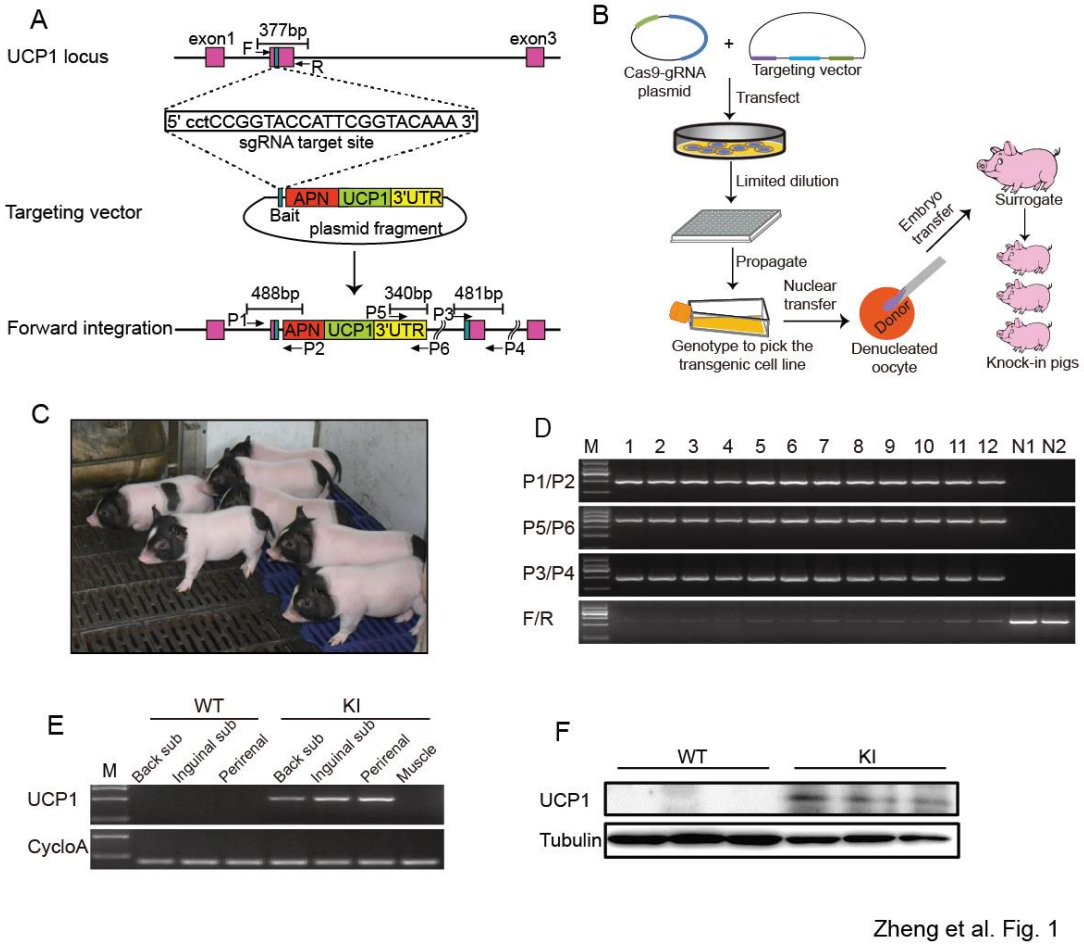

Zheng et al. Fig. 1

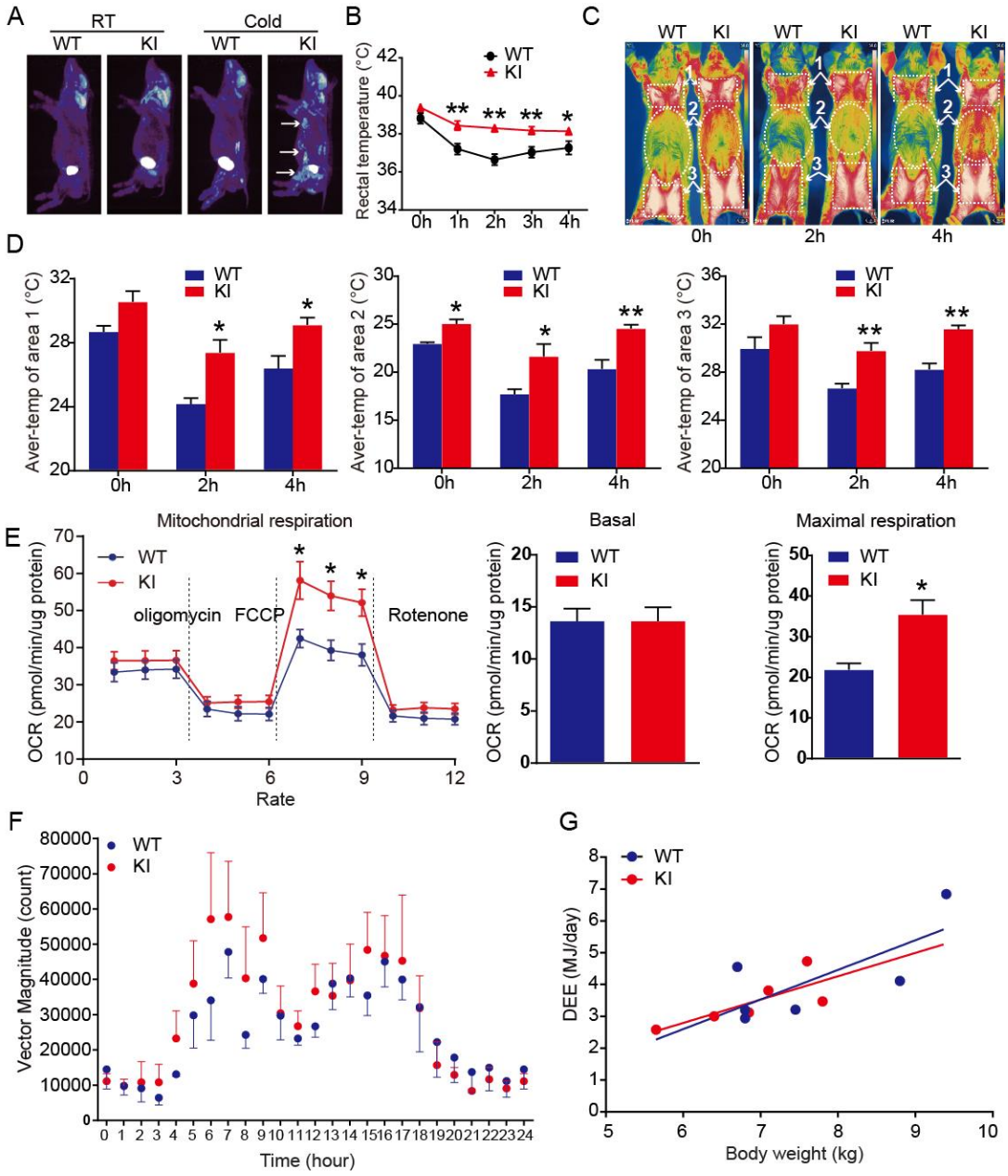

Zheng et al. Fig. 2

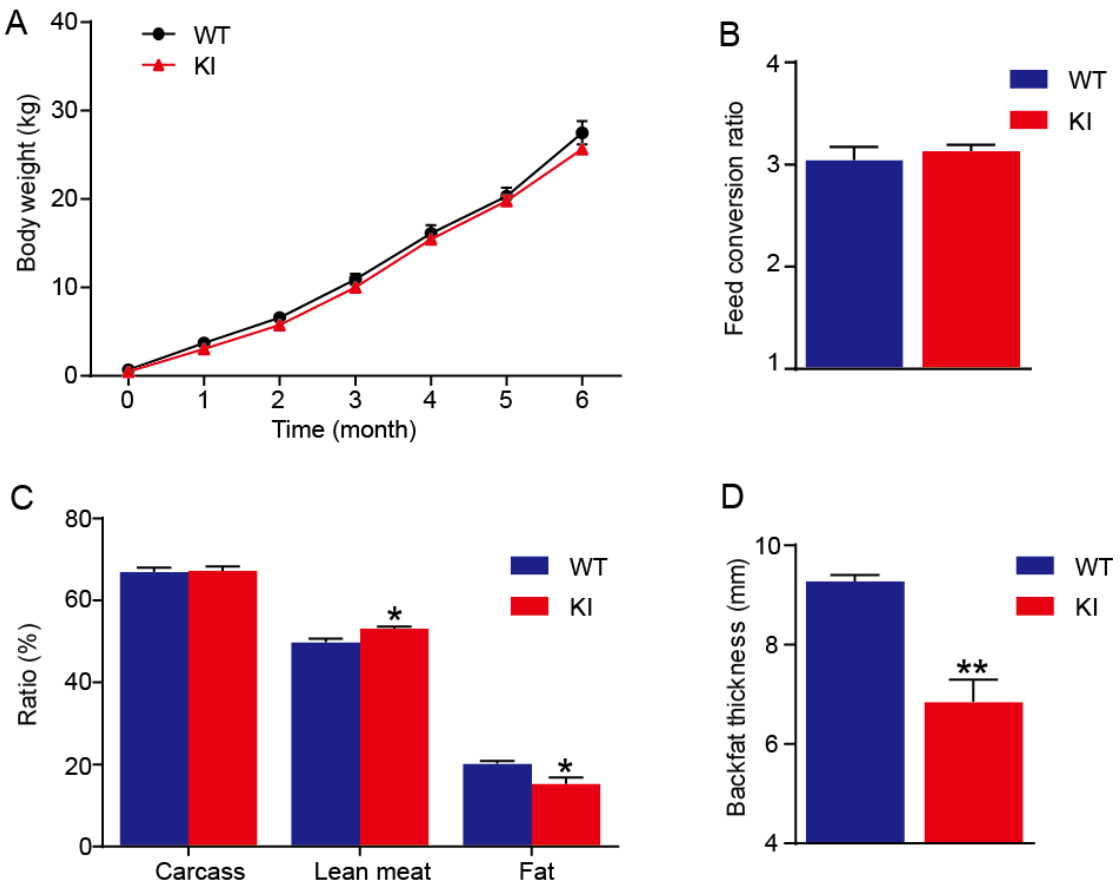

Zheng et al. Fig. 3

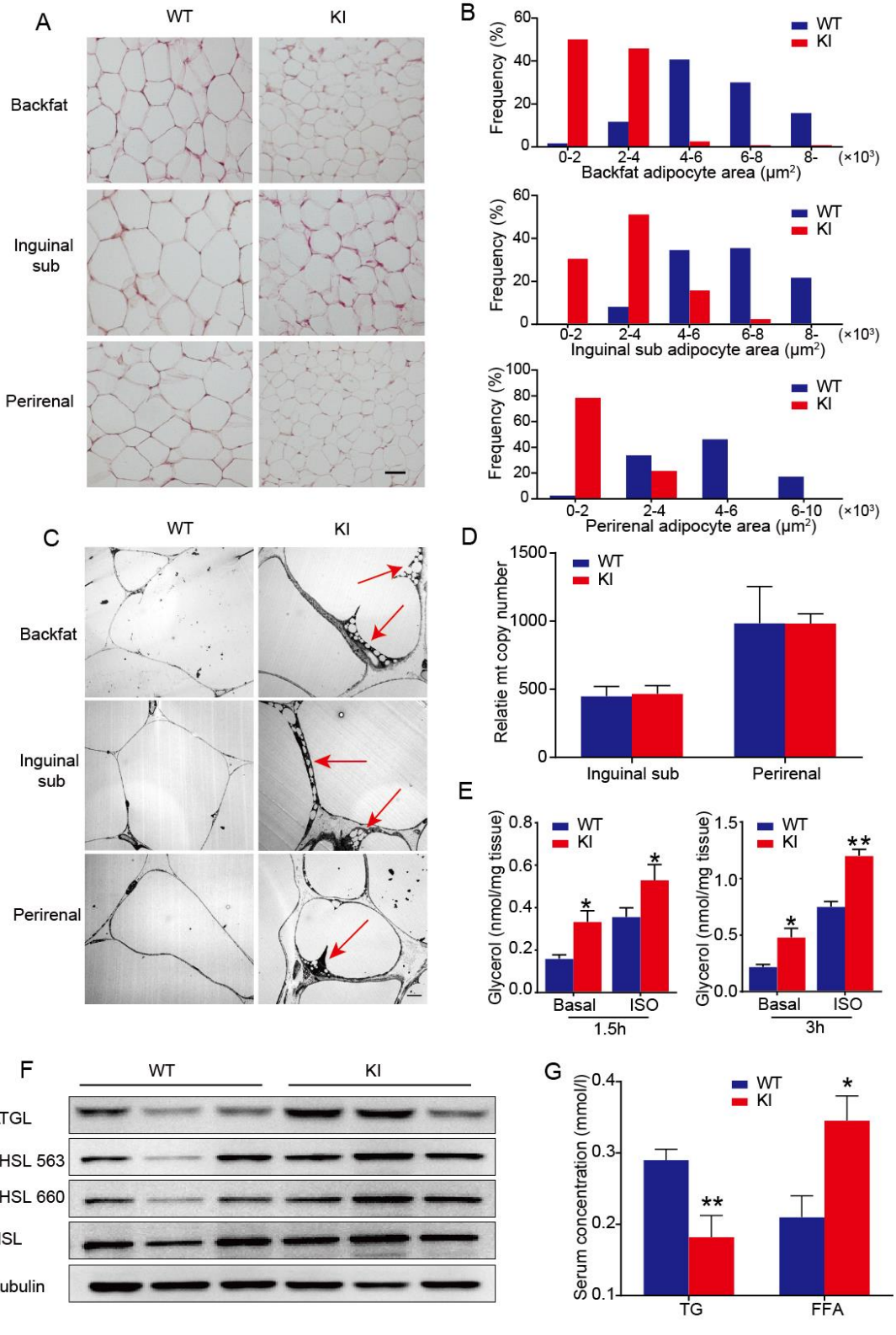

Zheng et al. Fig. 4

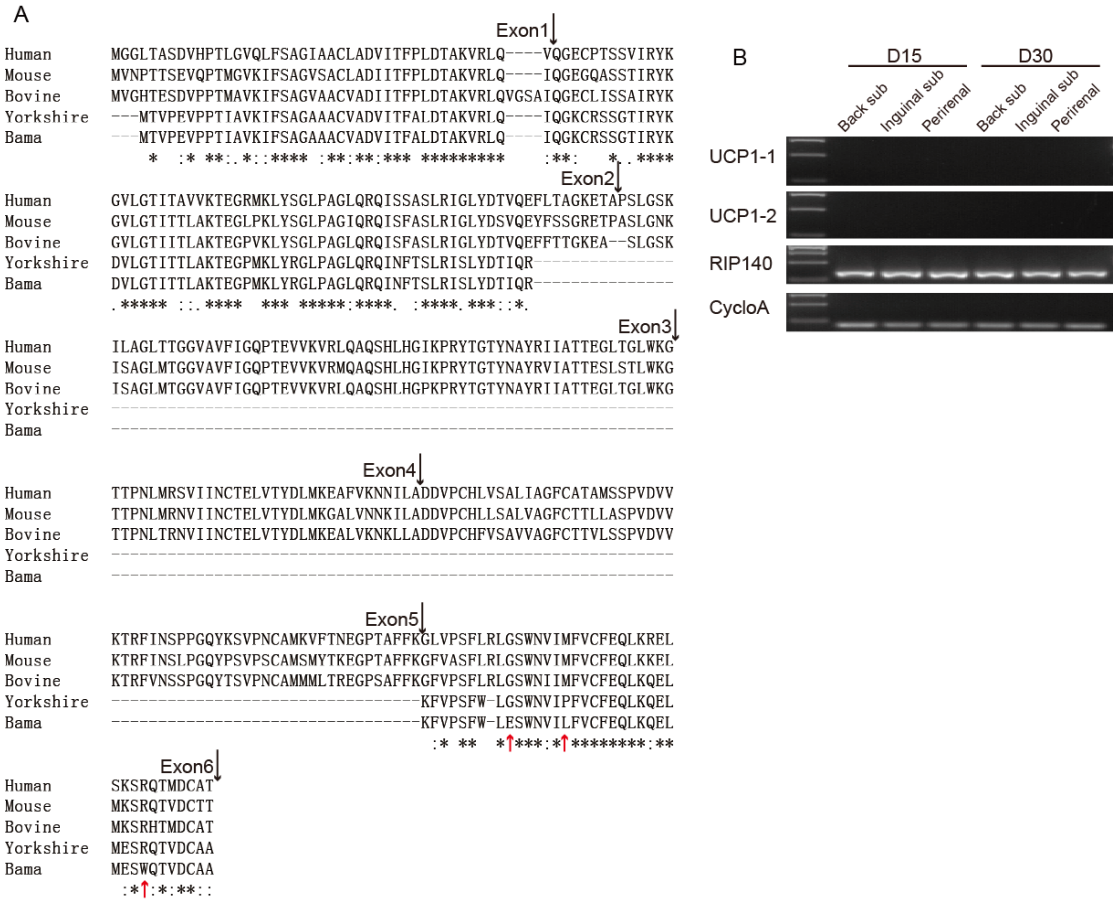

Zheng et al. Fig. S1

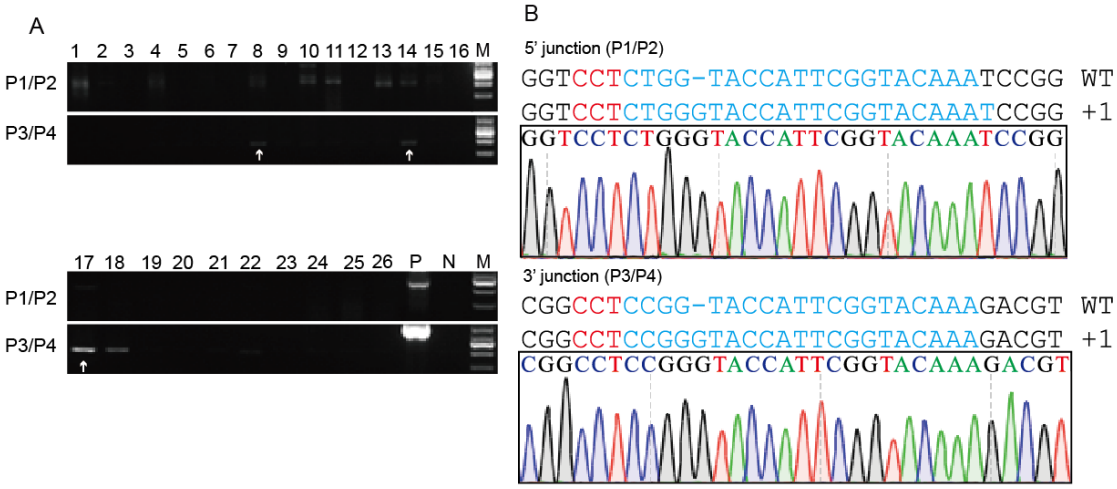

Zheng et al. Fig. S2

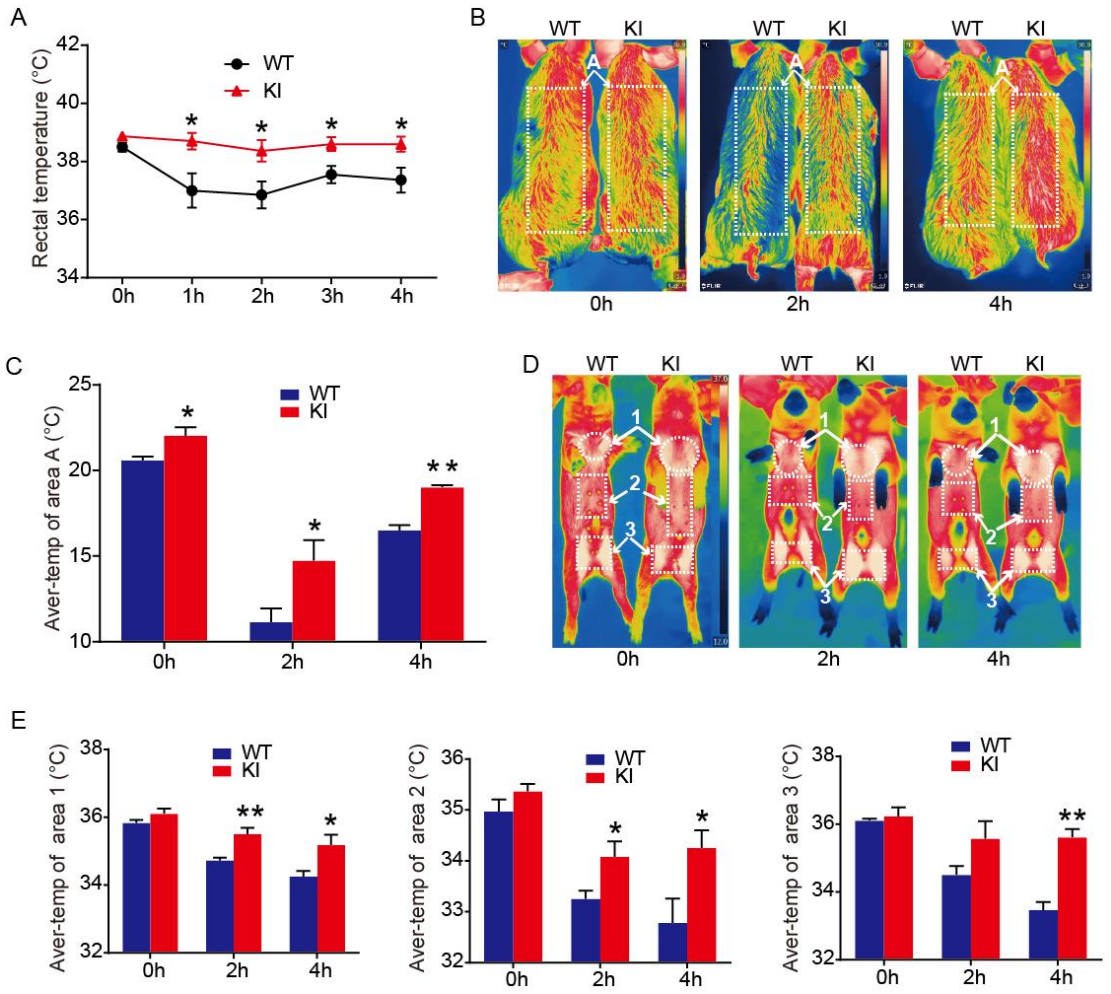

Zheng et al. Fig. S3

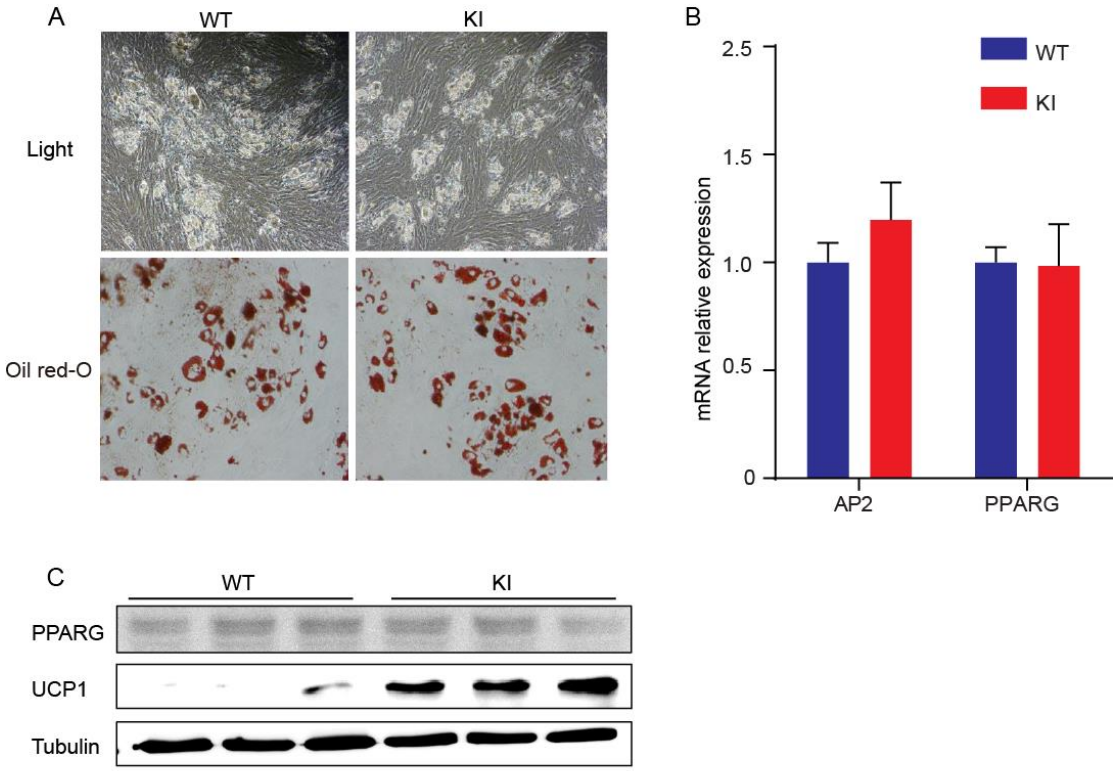

Zheng et al. Fig. S4

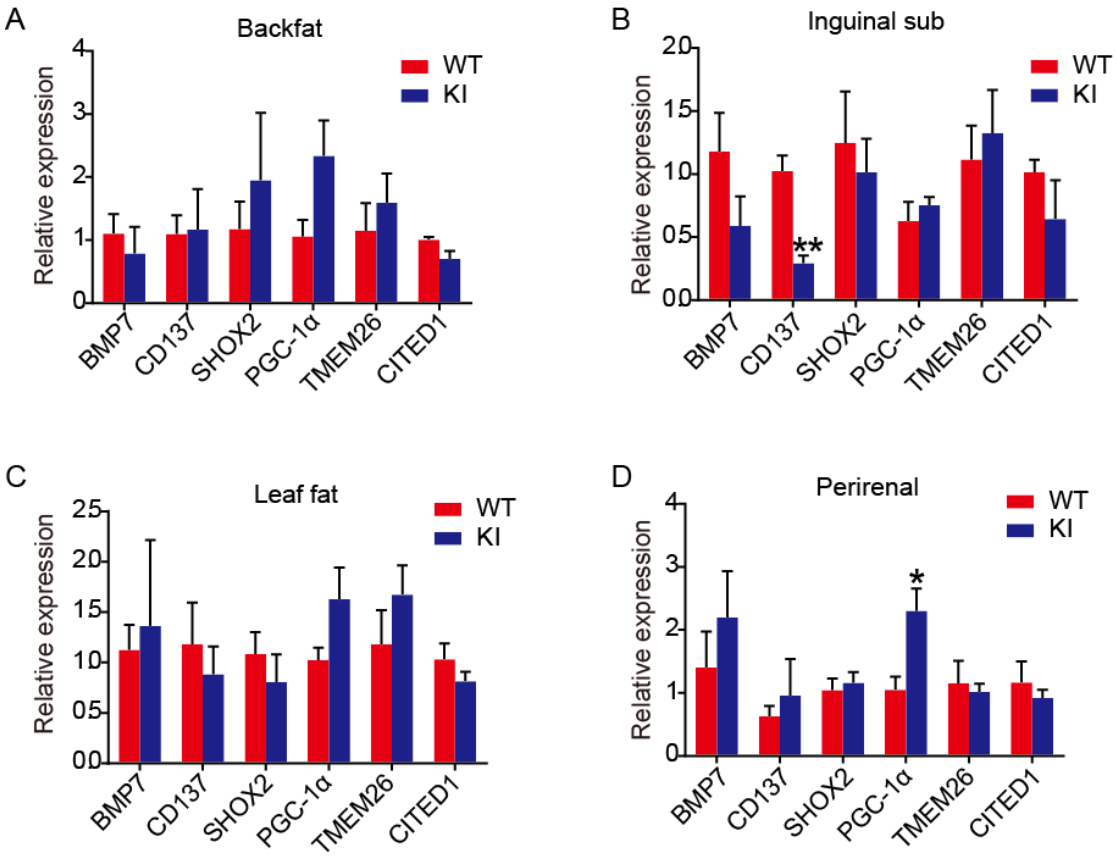

Zheng et al. Fig. S5

Supplementary Table 1. Genotyping of cell colonies

Clones genotyped	5' junction only	3' junction only	5' and 3' junction	KI efficiency (%)
26	8	1	3	11.54

Supplementary Table 2. Summary of nuclear transfer results from gene-targeted PEF

	Pig ID of surrogate	Embryos transferred	Pregnancy	Piglets at birth	KI	Survived for 1 month
	1230803	170	yes	2	yes	0
	1322706	184	no	-	-	-
	1224804	150	yes	8	yes	7
	1227503	220	yes	2	yes	1
	1238101	230	no	-	-	
	1220002	182	no	-	-	-
	1239201	185	no	-	-	-
	1223605	183	no	-	-	-
	1217302	195	no	-	-	-
	1313607	200	no	-	-	-
	1424501	190	no	-	-	-
	1222702	226	no	-	-	-
	1217703	238	no	-	-	-
Total number	13	2553	3	12	12	8

Supplementary Table 3. Growth performance and carcass traits between WT and KI pigs

	Genotype		
Trait	WT	KI	P-value
BW(kg)	27.11±4.44	24.13±1.43	0.2369
ADG(kg/d)	0.19±0.04	0.18±0.01	0.3857
CW(kg)	18.13±3.09	16.25±1.27	0.2888
%CW(g/100g of BW)	66.87±2.84	67.31±1.96	0.7969
BMSFW(kg)	8.30±1.38	7.45±0.46	0.2744
LMW(kg)	4.15±0.87	3.96±0.30	0.6845
%LMW(g/100g of BMSFW)	49.74±2.43	53.12±1.01	0.0318
FW(kg)	1.69±0.40	1.15±0.29	0.0495
%FW(g/100g of BMSFW)	20.17±1.80	15.28±3.11	0.0129
LFW(kg)	0.46±0.10	0.31±0.12	0.0568
%LFW(g/100g of BW)	1.69±0.12	1.27±0.45	0.0570
SW(kg)	1.27±0.18	1.16±0.07	0.2688
%SW(g/100g of BMSFW)	15.67±1.15	15.59±1.05	0.9187
BoW(kg)	1.18±0.07	1.18±0.15	0.9991
%BoW(g/100g of BMSFW)	14.97±3.70	16.01±3.13	0.6570
BT(mm)	9.28±0.25	6.84±0.90	0.0020**
LMA(cm^2)	15.45±1.07	17.33±1.61	0.1005

BW, body weight; ADG, average daily gain; CW, carcass weight; BMSF, sum of bone, lean muscle, skin and fat; LMW, lean meat weight; FW, fat weight; LFW, leaf fat weight; SW, skin weight; BoW, bone weight; BT, backfat thickness; LMA, longissimus muscle area.

Quantitative data are presented as mean±s.e.m. Significance was established using a 2-tailed Student's t-test. Differences were considered significant at $P<0.05$, **$P<0.01$.

Supplementary Table 4. A list of primers for Semi and Quantitative PCR

Gene	Forward	Reverse
UCP1	CACGGGGACCTACAATGCTT	GGTACGCTTGGGTACTGTCC
UCP1-1	CAAAGTCCGGCTACAGATCCA	GCAAAGACAGAAGGGCCAATG
UCP1-2	TCACCTCTCTTAGGATCAGCC	GTTGATGGAGTCACGGCAGA
RIP140	ATCAGGCAGCGAGTGAAAGACTTG	AGGAACGAGACCCATTGGACTTTG
CycloA	GCACTGGTGGCAAGTCCAT	AGGACCCGTATGCTTCAGGA
BMP7	CATGGTCATGAGCTTCGTCAAC	GTCCTTGTAGATGCGGAATTCAGC
CD137	AGAGGACAAGATCAGTGCCG	TGTCCACTTGTGCTGGAGAA
SHOX2	CTGTCCGAGGCCCGAGT	CGCCTGAACCTGCTGAAATG
PGC-1α	GTCCTTCCTCCATGCCTGAC	TGGTTTGCATGGTTCTGGGT
TMEM26	GGCGCTGACCCTCAAATACA	TTGCTGCTGGTATTTTGCGAC
CITED1	TGAGCTGCCGAGAGGAGG	AATTGGTGGGAGGTGTTGCT
AP2	GGTTACGGCTTCTTTCTCACC	CAAAGCCCACTCCCACTTCTT
PPARG	CCAGCATTTCCACTCCACACTA	GACACAGGCTCCACTTTGATG